

# Chapter 4

## Crystallization of Continuing Wave Laser Applications for Low-Temperature Polycrystalline Thin Film Transistors

### 4.1 Introduction



Low temperature poly-silicon TFTs fabricated by excimer laser annealing (ELA) had been applied to high performance AMLCDs and AMOLEDs. High quality displays with the peripheral integrated circuits had been proposed in recent year. Since the device driving capability would crucially influence the performance of the integrated circuits, the mobility of the device became a significant problem. According to the previous report, the mobility would be limited to a saturation value due to other effects, such as grain size, and surface roughness of poly-silicon. One solution was to substitute laser system with higher mobility for the poly-silicon active layer. At present, the most possible laser system was continuing wave laser. Owing to the crystallization film characteristics of Raman spectrum was same as silicon, as shown in Fig. 4-1 and 4-2, somewhat different was Raman shift that caused by micro-crystal or thermal stress. In the previous chapter, we had demonstrated that poly-silicon TFTs

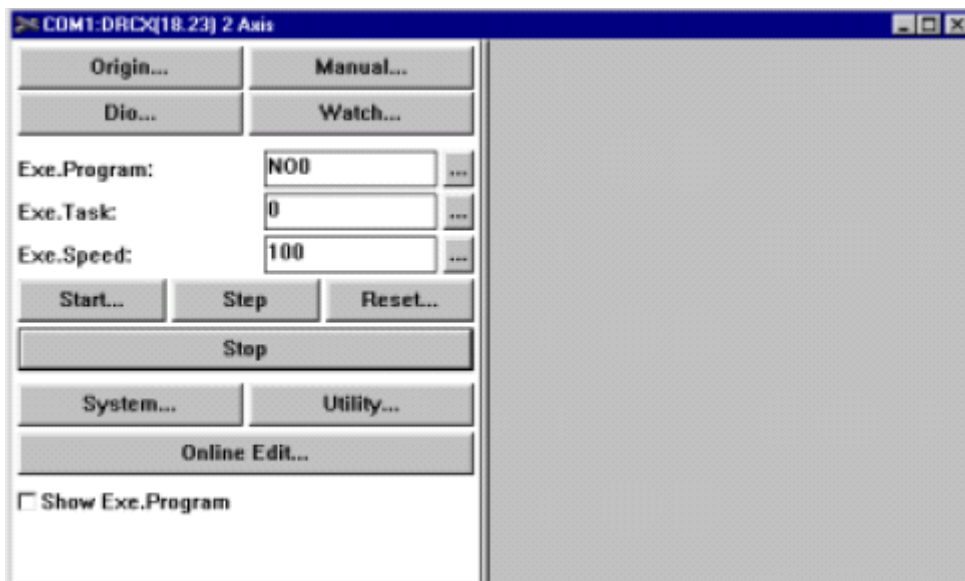
fabricated by direct laser crystallization of  $\alpha$ -silicon thin film with surface oxidation treatment would get normal mobility, including small grain size and more grain boundary. A novel crystallization technology of poly silicon thin film would be fabricated by continuing wave laser. It had pumping system that utilized Nd-YVO<sub>4</sub> (Yttrium Vanadate) crystal. This crystal had been growing in popularity because of it was high gain, low threshold, and high absorption coefficients at pumping wavelengths, which result from the excellent fit of the neodymium dopant in the crystal lattice. These advantages make Nd:YVO<sub>4</sub> a better choice than Nd:YAG for low-power devices such as hand-held pointers, and others compact lasers. The specifications of Nd-YVO<sub>4</sub> crystal had Nd dopant concentration 0.2 ~ 3 atm%; Dopant tolerance within 10% of concentration; Length 0.02 ~ 20mm; Coating specification HR @ 532 nm, R>99%; Orientation a-cut crystalline direction (+/-5°C); Wavefront distortion < $\lambda$ /8 at 633nm; Parallelism < 10 arc seconds; Perpendicularity < 5 arc minutes; Surface flatness < $\lambda$ /10 at 632.8nm; Clear aperture Central 95% and Damage threshold over 15J/cm<sup>2</sup> (rods without coating) over 700 MW/cm<sup>2</sup> (coating). High power, continuing wave, single-frequency (532nm) Nd:YVO<sub>4</sub> laser was studied. The specifications of continuing wave laser have output power 10W; wavelength 532nm; line width < 5MHz; beam diameter 2.25mm +/-10%; beam divergence < 0.5mrad; pointing stability < 2umrad/°C; power stability +/-1%; noise < 0.03% rms and polarization vertical > 100:1. The large grain size about 3um in the active layer of poly-silicon TFTs that were fabricated by continuing wave laser crystallization in demonstrated excellent carrier mobility is proposed .

The scan system of the single axis servo motor was introduced with specification that was included the Repeatability, Maximum speed, Maximum load capacity, Rated thrust, Caution for maximum speed, Permissible overhang; Repeatability was determined as follows. Positioning operation to the specified point in one direction was repeated 30 times to obtain a standard deviation, which was then multiplied by 3. The maximum speed here means the

maximum carrying speed. Yamaha's single axis robots can carry the work at this speed regardless of their weight as long as it was within the maximum load capacity. If the carrying distance was short, however, the maximum speed may not be reached because the heavier the work being carried was, the more lenient the acceleration /deceleration curve becomes. The maximum load capacity means the maximum weight that could be loaded on the slider and carried. When selecting the model for use, the total weight of tools being used (air cylinder, chuck, etc.) and the work should be less than this value. If the gravity center of the work was offset from the center of the slider, it was necessary to consider the permissible overhang as well. Also, it was so designed that optimum acceleration/deceleration speed and servo parameters were automatically set only by entering the total weight of tools and work for the load capacity parameter on the controller. The rated thrust means the force applied in the advancing direction of the slider while it was held stationary. During the vertical use (a force was applied downward from the top), reduce the weight of the load. When the slider moves and only at a slow speed (about 10% of the maximum speed), this value may become lower than the specification. Also, the type B who was driven by the timing belt cannot be used for the purpose where thrust was applied. When the unit was a ball screw drive type and had a long stroke, operation at the maximum speed may be accompanied with abnormal noise and vibration because of resonance of the ball screw. In such a case, reduce the speed to the level described in the note section. (It was possible either to reduce the carrying speed in the entire program or to adjust it for each command for movement.) The permissible overhang means how much the work may overhang. It was indicated as a specification by the distance from the center of the top face of the slider to the gravity center of the work to be carried by the weight. This value was determined on the basis of the service life of the linear guide. Under normal operation conditions, the 90% service life of the linear guide was 10,000km (5,000km for T4 and T5) or more if gravity centers of the work and tools are kept within the permissible overhang. When using the unit with the overhang exceeding the specification data, add a

separate support guide so that no load was applied to the linear guide of the single axis robot [22].

The software operation was introduced by using POPCOM Windows; the operation method was included the 1.connect a robot controller; [Robot Operate] window was needed to operate or observe status of robots connected to robot controller; 2. [Robot Operate] window was shown.



3.The recipe was selected by “Exe.Program” and speed was adjusted by “Exe.Speed”, 4.to push the start button [23].

## 4.2 Experimental Procedure

### 4.2.1 Speed Constant for Scanning

A buffer layer of 50nm/150nm thickness of SiN<sub>x</sub>/SiO<sub>x</sub> were deposited by plasma enhanced chemical vapor deposition (PECVD) means at 450°C on glass substrate. Amorphous silicon film of a 50nm thickness was deposited on buffer layer as the active layer by PECVD at 500°C with SiH<sub>4</sub> gas source then was heated at 500°C for one hour to remove the incorporated hydrogen in the film. After dehydrogenation, first procedure was prior clean

treatment with HF 1% clean for 30seconds, and then O3 water 20ppm clean for 100seconds. Crystallization was carried out by a continuing wave laser with wavelength of 532 nm in atmosphere at room temperature. The scan system was included the single axis servo motor, software for speed controlling and black stage for holding the substrate. The optical system was including the focus lens with the focus 600mm and one reflect lens. All of systems were shown in Fig. 4-3. The scan speed was fixed at 2.5cm/sec then the power of CW laser was adjusted for every parameters of experiment. It was included the laser power 1W, 2W, 4W, 6W and 8W. After laser irradiation, top-gate, poly-silicon TFTs was fabricated with conventional processing, as shown in Fig. 4-4, the polycrystalline layer was tailored into active islands. Next, PR coating and patterned then n+ ion doping of PH<sub>2</sub><sup>+</sup> ion implantation with the concentration of 6×10<sup>14</sup> cm<sup>-2</sup>, then 1000Å thick TEOS gate oxide was deposited using PECVD, then PR coating and patterned, then LDD ion doping of PH<sub>2</sub><sup>+</sup> ion implantation with the concentration of 2×10<sup>13</sup> cm<sup>-2</sup> was carried out to form the n-type source and drain region, then PR coating and patterned, then p+ ion doping of BF<sub>2</sub><sup>+</sup> ion implantation with the concentration of 1×10<sup>15</sup> cm<sup>-2</sup> was carried out to form the p-type source and drain region, than rapid thermal annealing was performed to activate the implanted dopants and recrystallize the source and drain region at temperature 350°C. 2000Å thick Mo gate electrode was deposited using PVD system, then a 3000Å/500Å thick PECVD SiO<sub>x</sub>/SiN<sub>x</sub> was deposited as passivation layers. After contact holes opening, Ti/Al/Ti was deposited by PVD system and patterned to form the source and drain contact pads.

The grain size of the CW poly-silicon thin film could be measured by using Scanning electron microscope (SEM) for distinguishing the individual grain structure. The transfer characteristics of the poly-Silicon TFTs were measured by HP4156 semiconductor parameter analyzer. The device parameters including the field-effect mobility, the threshold voltage, the subthreshold swing, the OFF current and ON/OFF current ratio were extracted from the measured characteristics.

#### 4.2.2 Power Constant for CW Laser

The power of CW laser was fixed in 1.5, 3, 4 and 8W, respectively, then the scan speed was adjusted for every parameters of experiment. It was included the scan speed range from 1 to 32cm/sec. After laser irradiation, top-gate, poly-silicon TFTs was fabricated with conventional processing flow was same as speed constant for scanning condition.

#### 4.2.3 Back Side Irradiation and Power Constant for CW Laser

The power of CW laser was fixed in 4W then the scan speed was adjusted for every parameters of experiment. It was included the scan speed 7, 10, and 12cm/sec. The substrate backside was irradiated by continuing wave laser. After laser irradiation, top-gate, poly-silicon TFTs was fabricated with conventional processing flow was same as speed constant for scanning condition.



### 4.3 Results and Discussion

#### 4.3.1 Physical Characterizations of CW Poly-Silicon Thin Film

The grain size of the CW poly-Silicon thin film could be measured by using SEM. In order to distinguish the individual grain structure, the CW poly-silicon thin film was immersed in the Secco etching solution, which etched the grain boundaries more quickly than the interior parts of the grains. In the Fig. 4-5~4-9 were shown the SEM micrographs of the CW poly-silicon film after Secco etching for 60seconds. The CW laser power was adjusted to partially or completely melt the  $\alpha$ -silicon thin film. In addition, different laser power had influence the dimension on poly crystallization. In the Fig. 4-5, the applied laser power was 1W and scan speed was constant for 2.5cm/sec, the poly crystallization film of CW laser was distinguished three parts that were partial melting, complete melting and nearly complete

melting, it was observed the center area of poly crystallization film that was partial melting region with the fine grain, but the drawing of edge position had different grain structure, owing to the laser beam edge with low energy, so the grain structure was existed the poly silicon and  $\alpha$ -silicon in this region. The applied laser power was 2W and scan speed was constant with 2.5cm/sec, as shown in Fig. 4-6, the partial melting and complete melting region with diameter 168 $\mu$ m, center area of poly crystallization film that was complete melting region with the broken hole of poly crystallization film, because of the film absorbed the laser energy to exceed complete melting energy and heating dispersed too slowly in the  $\alpha$ -silicon film. The middle-melting region was near the broken hole where had the larger grain size about 1 $\mu$ m. The partial melting region was removed from the center position where had the fine grain in this area. The applied laser power was 4W and scan speed was constant at 2.5cm/sec, as shown in the Fig. 4-7, the partial melting and complete melting region with diameter 234 $\mu$ m, the laser power was more high the diameter of partial melting and complete melting region was more broad but the broken hole of poly crystallization film was larger so the laser power was increased to exceed the 2W and scan speed is constant at 2.5cm/sec, the  $\alpha$ -silicon film was broken. In the Fig. 4-8, it was shown the partial melting and complete melting region with diameter 250 $\mu$ m, In the Fig. 4-9, it was shown the partial melting and complete melting region with diameter 258 $\mu$ m and white point was broken hole with substrate and film. In this condition of constant speed 2.5cm/sec was not found the large grain size and usable poly crystallization film.

In the power constant condition of poly crystallization thin film was measured by using SEM. The poly crystallization regions were defined three regions that were same as before mentions about constant scan speed at 2.5cm/sec. The complete melting and nearly complete melting region was name the “a”. In the constant laser power is 1.5W and scan speed was 1 cm/sec, as shown in Fig. 4-10, the grain size of area “a” was about 1.2 $\mu$ m, the distance of “a” was 50 $\mu$ m, and the total region of poly crystallization distance was 178 $\mu$ m, the far from “a”



was the fine grain. In the Fig. 4-11, the constant laser power is 1.5W and the scan speed was 3 cm/sec, the grain size of area “a” was about 0.6 $\mu$ m, the distance of “a” was 40 $\mu$ m, and the total region of poly crystallization distance was 165 $\mu$ m, the far from “a” was the fine grain size. In the Fig. 4-12, the constant laser power was 1.5W and the scan speed was 5 cm/sec, the grain size of area “a” is about 0.3 $\mu$ m, the distance of “a” was 15 $\mu$ m, and the total region of poly crystallization distance was 130.5 $\mu$ m, the far from “a” was the fine grain. In the Fig. 4-13, the constant laser power was 1.5W and the scan speed was 7 cm/sec, the grain size of center area was about 0.005 $\mu$ m, the distance of “a” was disappearing, and the total region of poly crystallization distance was 118.8 $\mu$ m. In this condition of constant power 1.5W was not found the large grain size. But it was observed the region “a” variation was relation with scan speed, the scan speed was increased the region of “a” would be decreased.

The laser power was varied to 3W and scan speed was varied from 5 to 6cm/sec, in the Fig.4-14, the scan speed was 5cm/sec and constant laser power was 3W, the substrate had to be broken under the buffer layer. The total region of poly crystallization distance was 150.0 $\mu$ m. In the Fig.4-15, the scan speed was 6cm/sec and constant laser power was 3W, the grain size of area “a” was about 0.6 $\mu$ m, the distance of “a” was 45.0 $\mu$ m, and the total region of poly crystallization distance was 130.5 $\mu$ m, the far from “a” was the fine grain size.

The laser power was varied to 4W and scan speed was varied from 6 to 7cm/sec, in the Fig.4-16, the scan speed was 6cm/sec and constant laser power was 4W, the center area of poly crystallization film that was complete melting region with the broken hole of poly crystallization film, the grain size of near broken hole was about 3 $\mu$ m, the distance of “a” was 75.0 $\mu$ m, the total region of poly crystallization distance was 139.5 $\mu$ m. In the Fig.4-17, the scan speed was 7cm/sec and constant laser power is 4W, the grain size of area “a” was larger than 3 $\mu$ m, the distance of “a” was 56.3 $\mu$ m, and the total region of poly crystallization distance was 132.0 $\mu$ m, the far from “a” was the fine grain size.

When the laser power was varied to 8W and scan speed was varied from 7 to 32cm/sec,



in the Fig. 4-18 (b), the scan speed was 7cm/sec and constant laser power was 8W, the center area occurred the broken hole of poly crystallization film, the distance of “a” was 98.4um, the total region of poly crystallization distance was 153.8um. In the Fig. 4-18 (a), the scan speed was 10cm/sec and constant laser power was 8W, the center area condition was same as Fig. 4-18 (b), the distance of “a” was 79.7um and the total region of poly crystallization distance was 142.5um, the far from “a” was the fine grain size. In the Fig. 4-19, the condition was same as Fig.4-18 (b), the distance of “a” was 63.8um; the total region of poly crystallization distance was 126.8um. In the Fig.4-20, the scan speed was 14cm/sec and constant laser power was 8W, the grain size of area “a” was larger than 3um, the distance of “a” was 41.3um, and the total region of poly crystallization distance was 125.3um, the far from “a” was the fine grain size. In the Fig. 4-21, the scan speed was 16cm/sec and constant laser power was 8W, the grain size of area “a” was larger than 3um, the distance of “a” was 39.6um, and the total region of poly crystallization distance was 120.0um, the far from “a” was the fine grain size. In the Fig. 4-22, the scan speed is 32cm/sec and constant laser power was 8W, the grain size of area “a” was larger than 3um, the distance of “a” was 30.0um, and the total region of poly crystallization distance was 105.0um, the far from “a” was the fine grain size. In this condition of constant power that was included the 3, 4 and 8W was found the large grain size and usable poly crystallization film. It was observed the region “a” variation was relation with scan speed and laser power, first, the scan speed was increased the region of “a” will be decreased; second, the laser power was increased the region of “a” would be increased. The broken hole occurred in constant power 3W and scan speed less than 5cm/sec; constant power 4w and scan speed less than 6cm/sec; constant power 8W and scan speed less than 12cm/sec. The large grain size and usable poly crystallization were not found in low laser power, the large grain size region wider was better, so the optimization condition was laser power 4W and scan speed 7cm/sec.

As a result of large grain size and large distribution needed for usable poly crystallization,

the backside irradiation of substrate was investigated to get the better condition, the constant power 4W and scan speed was varied from 7 to 12cm/sec, in the Fig. 4-23, the scan speed was 7cm/sec and constant laser power was 4W, the center area occurred the broken hole of poly crystallization film, the distance of “a” was 82.5um, the total region of poly crystallization distance was 144.0um. In the Fig. 4-24, the scan speed was 10cm/sec and constant laser power was 4W, the grain size of area “a” was larger than 3um, the distance of “a” was 67.5um, and the total region of poly crystallization distance was 142.5um, the far from “a” was the fine grain size. Fig. 4-25, the scan speed was 12cm/sec and constant laser power was 4W, the grain size of area “a” was small than 1um, the distance of “a” was 67.5um, and the total region of poly crystallization distance was 130.5um. The better condition of backside irradiation of substrate was obtained to utilize the constant power 4W and the some heating was absorbed and reserved by substrate, this mechanism slowed down the super cooling taking place before the onset of solidification due to homogeneous nucleation. So the large grain distribution was wider than front side irradiation.

In the Fig 4-26(a) was the high-magnification cross-sectional TEM image and Fig 4-26(b) was electron diffraction pattern of CW laser crystallite. The diffraction pattern reveals that the crystallite exhibits  $\langle 111 \rangle$  orientation along the direction of film grain growth, The TEM image was shown the large grain and grain boundary was different from excimer laser crystallite so the Raman shift caused by thermal stress.

#### **4.3.2 Electrical Characterizations of CW Poly-Silicon TFTs**

According to the physical characterizations in the previous section, it was noticed that the CW poly-silicon thin film exhibited two optimization conditions, such as front side irradiation with constant power 4W and scan speed 7cm/sec; back side irradiation with constant power 4W and scan speed 10cm/sec. In the active layer, it had been demonstrated that carrier mobility could be effectively enhanced by suitably controlling the grain size. To

take the advantage of carrier enhancement for large grain poly crystallization thin films, it was fabricated by the continuing wave laser was good method.

The file transfer characteristics of CW LTPS TFT using front side irradiation with constant power 4W and scan speed 7cm/sec. Some important electrical characteristics of LTPS TFTs were also listed, it was included the  $W/L = 6\mu\text{m}/12\mu\text{m}$ ,  $V_d=0.1\text{V}$ ,  $V_t(\text{p}1) -4.0\text{V}$ ,  $V_t(\text{p}2) -4.2\text{V}$ ,  $U_{fe}(\text{p}1) 206 \text{ cm}^2/\text{V}\cdot\text{sec}$ ,  $U_{fe}(\text{p}2) 227 \text{ cm}^2/\text{V}\cdot\text{sec}$ ,  $I_{off}(\text{p}1) 2.00\text{E}-14\text{A}$ ,  $I_{off}(\text{p}2) 1.87\text{E}-13\text{A}$ ,  $SS(\text{p}1) 0.46$ ,  $SS(\text{p}2) 0.41$  for p-type, as shown in Fig. 4-27 and  $W/L = 6\mu\text{m}/12\mu\text{m}$ ,  $V_t(\text{n}1) 7.6\text{V}$ ,  $V_t(\text{n}2) 7.3\text{V}$ ,  $U_{fe}(\text{n}1) 298 \text{ cm}^2/\text{V}\cdot\text{sec}$ ,  $U_{fe}(\text{n}2) 257 \text{ cm}^2/\text{V}\cdot\text{sec}$ ,  $I_{off}(\text{n}1) 2.05\text{E}-13\text{A}$ ,  $I_{off}(\text{n}2) 1.72\text{E}-13\text{A}$ ,  $SS(\text{n}1)$  and  $SS(\text{n}2) 0.37$  for n-type, as shown in Fig. 4-28.

#### 4.4 Summary

Crystallization of amorphous silicon ( $\alpha$ -silicon) thin films were utilized by CW lasers of wavelength 532nm with different power and scan speed. It included the speed control in stage with different power during laser scanning; front and backside scan on substrate at different scanning speed. Owing to the laser beam energy distribution was the Gauss shape and laser beam size was affected by focus lens and laser power, we employed the focus lens with focus 600mm and focus the laser beam on substrate where the beam diameter was about 300um, when laser power more high the diameter more broad. It was observed the region “a” that was included complete melting and partial melting region, variation was relation with scan speed and laser power, first, the scan speed was increased the region of “a” would be decreased; second, the laser power was increased the region of “a” would be increased. The broken hole occurred in constant power 3W and scan speed less than 5cm/sec; constant power 4W and scan speed less than 6cm/sec; constant power 8W and scan speed less than 12cm/sec. The large grain size and usable poly crystallization were not found in low laser power, the large grain size region wider was better, so the optimization condition was laser power 4W and scan speed 7cm/sec. The better condition of backside irradiation of substrate was obtained to

utilize the constant power 4W and the some heating was absorbed and reserved by substrate, this mechanism slowed down the super cooling taking place before the onset of solidification due to homogeneous nucleation. So the large grain distribution was wider than front side irradiation. The LTPS thin films were fabricated by CW laser with grain size more than 3 $\mu$ m, grain shape like long bulk and large grain was aggregated in “a” on crystallization surface and the LTPS TFTs fabricated at large grain size area, the field effect mobility of 298 and 210  $\text{cm}^2/\text{V}\cdot\text{s}$  can be achieved for n-channel and p-channel LTPS TFTs, respectively. The thresholds voltage was shifted to 7V and  $-4\text{V}$  for n-channel and p-channel LTPS TFTs, respectively. Owing to the crystallization ambience was atmosphere. In the future work, the continuing waves laser crystallization in the ambience of low  $\text{O}_2$  concentration will improve the electric characters of thresholds voltage.

